Available online at www.CivileJournal.org

Civil Engineering Journal

(E-ISSN: 2476-3055; ISSN: 2676-6957)

Vol. 9, No. 12, December, 2023

Effect of Infills on the Response Modification Factor for Infilled Reinforced Concrete Frame Buildings

Dina Hesham Helmy [1*], Hussein Okail [2], Mostafa Zidan [3]

[1] *Structural Engineering and Construction Management Department, Faculty of Engineering & Technology, Future University in Egypt, Egypt.*

[2] *Department of Structural Engineering, Faculty of Engineering and Technology, Ain Shams University, Cairo, Egypt.*

[3] *Department of Civil Engineering, Faculty of Engineering and Technology, Ain shams University, Cairo, Egypt.*

Received 30 June 2023; Revised 13 October 2023; Accepted 09 November 2023; Published 01 December 2023

Abstract

RC frames with unreinforced masonry infill walls are the most common type of building. Unreinforced masonry walls are often not considered by engineers in the design process, although walls and frames interact during strong ground motion, leading to structural responses deviating radically from what is expected in the design. Under lateral load, reinforced concrete confining members (frames) act in tension or compression, depending on the direction of the lateral seismic pressures. Meanwhile, masonry walls act as diagonal struts prone to compression. This research aims to develop the effect of masonry infills and their distribution on the value of the resulting response modification factor. For this purpose, a parametric study was performed on five, seven, and ten-story' buildings modeled as bare and infilled frames. Infill ratio, panel aspect ratio, unidirectional eccentricity, and bidirectional eccentricities were the parameters investigated. Each proposed model's resulting response modification factor was compared to the value cited in different international codes. It was concluded that this value differs depending on several parameters and cannot be constant for a certain structural system. The novelty of this research is the deduction of a general equation to calculate the response modification factor as a function of the percentage of infills and the eccentricity, while presenting two different methods to calculate it.

Keywords: Diagonal Struts; Infill; Masonry; Response Modification; Seismic Performance.

1. Introduction

Reinforced concrete (RC) frames with unreinforced masonry infill walls are known as infilled RC frames [1, 2]. These buildings are among the most frequent low- to medium-rise structural forms seen worldwide. Infilled panels are used as partitions in structures with infilled frames, while the bounding frame serves as a structural skeleton to bear lateral and gravitational loads. Masonry structural walls [3] are frequently utilized by architects because of their aesthetic appeal and low labor cost [4, 5], but they also help to resist lateral loads like wind and seismic loads [6]. Design engineers disregard the impact of infills on the overall structural performance by considering them as non-structural components. As a result, the performance of infilled RC frames will not perform as expected given the structural assessments [7, 8]. However, there are differences between the structural behavior of infilled frames and bare frame structures [9, 10] because the presence of infills, both regularly and irregularly arranged infills, can significantly change the local stress distributions in the adjacent frame members and alter the overall structural dynamic behavior [11–13]. Additionally, under reversed cyclic loads, the brittle nature of masonry infill materials frequently imposes greater harm on the hysteretic behavior of structures and results in significant localized damage to the nearby braced structural parts. As a

* Corresponding author: dina.hesham@fue.edu.eg

http://dx.doi.org/10.28991/CEJ-2023-09-12-09

result, design engineers should include in their studies how infills as well as the ground motion duration [14] would affect the overall structural performance. In recent times, many studies have included the effect of the presence of infill walls on the seismic response of different buildings, but they did not discuss how the definition of the response modification factor as a constant in all building codes is too conservative.

In 2021, the infill wall interaction amplifying the torsional response of buildings at the bottom story was discussed [15], and it was proved that the infill walls have altered the load-resisting path and effectively enhanced the load redistribution ability for the frames [16, 17], depending on the construction sequences of the infilled frames [18]. Moreover, infill walls can contribute to a lateral strength increase of up to 60% compared to bare frames [19]. However, even with infills of uniform distribution, several low-rise frame types are vulnerable to the negative infill effect [20]. Furthermore, innovative systems were proposed to enhance the infill-column interaction, such as retrofitting the infill walls with highly ductile concrete layers in 2022 [21–23].

This study describes an analytical method used to evaluate the lateral load resistance of infilled reinforced concrete frame structures with various configurations [24, 25]. Furthermore, the seismic response modification factor for all buildings will be assessed in accordance with FEMA P-695 [26]. Then, an equation for calculating the ductility factor depending on the percentage of infills will be deducted for medium-rise infilled-frame buildings. Recently, the effect of infills on the response modification factor for infilled buildings was discussed, such as [27–32], case studies and experimental studies were presented [29, 33], and parametric studies were presented [28, 30, 34]. According to Scopus (May 2023), we searched related to (response AND modification AND factor AND buildings), 674 document results were selected. The history of publishing was presented in Figure 1, for the frequency of publication by year, and Figure 2, for the frequency of publication by country. The keywords were analyzed by VOSviewer software in Figure 3, and Tables 1 and 2 along with an example of the output are shown in Figure 4.

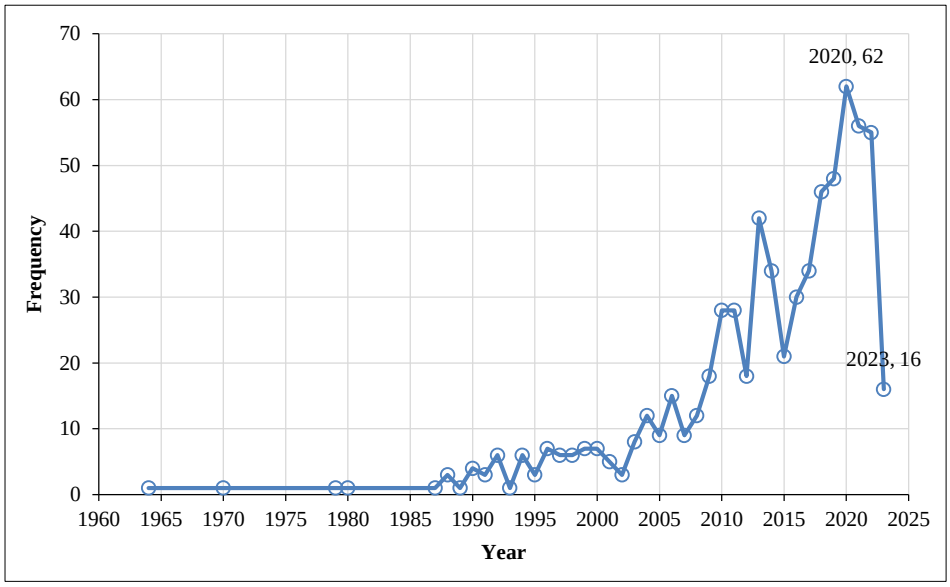

Figure 1. The frequency of publishing through the years

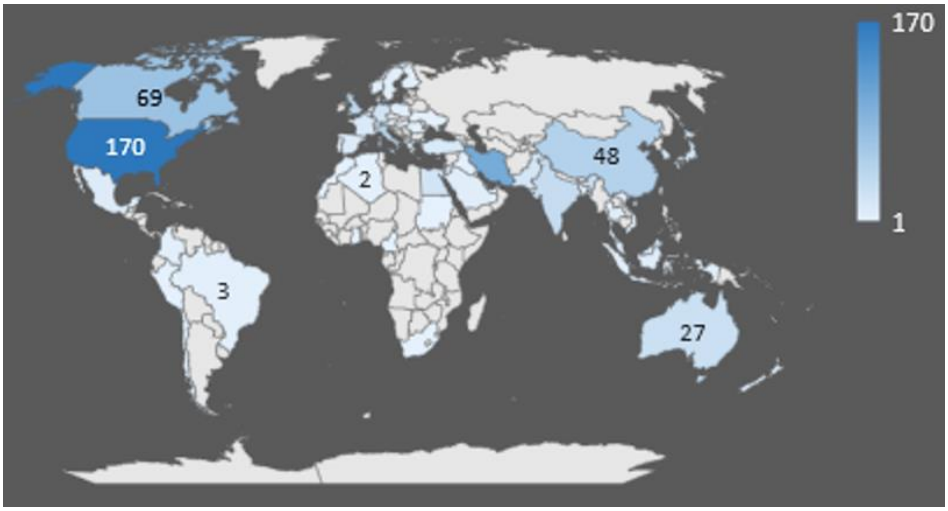

Figure 2. The frequency of publishing in different countries

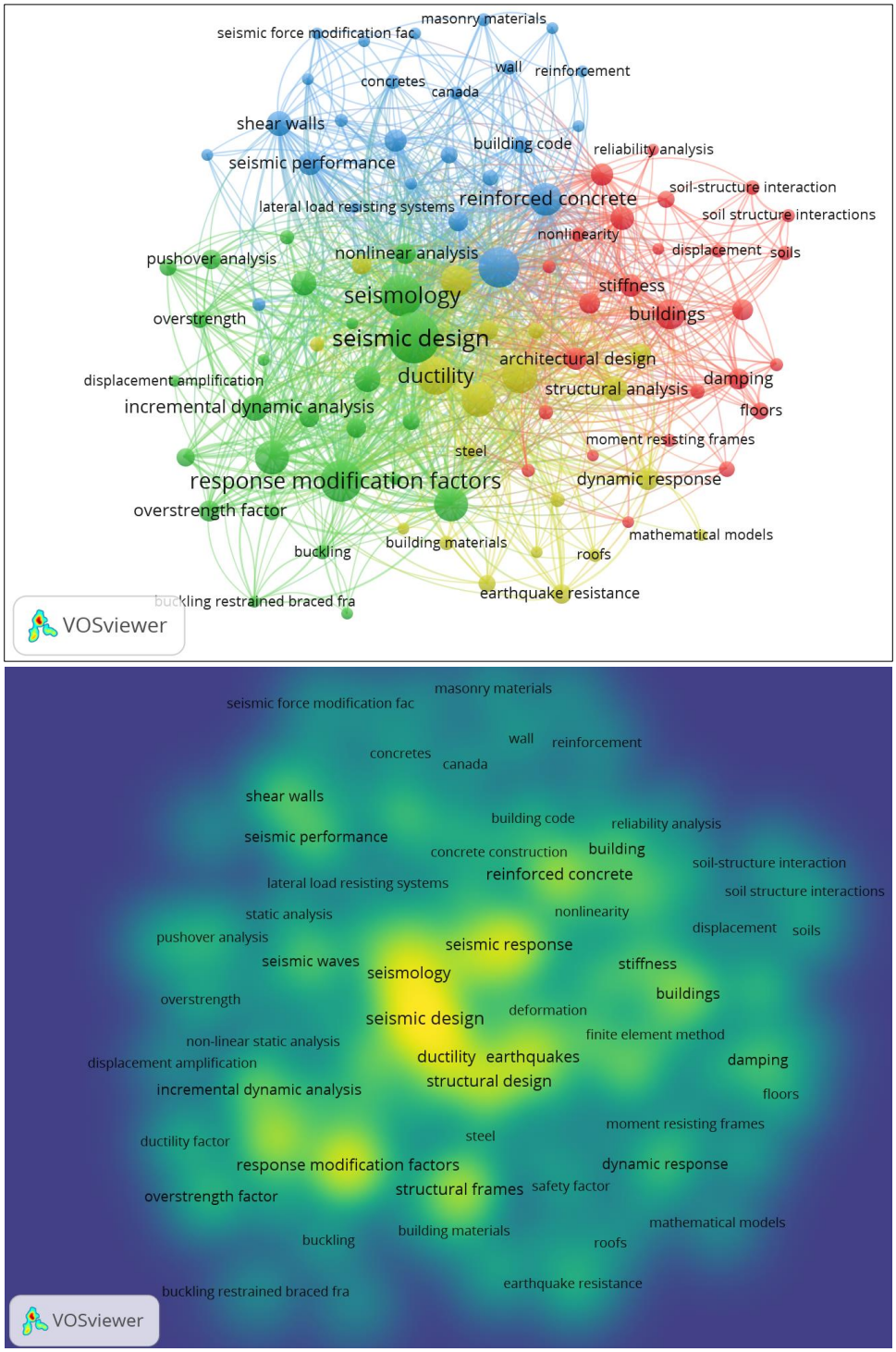

Figure 3. Visualization of the keyword's links

Table 1. The occurrences of each keyword and their total link of strength

Keyword	Occurrences	Total Link of strength
Seismic design	178	1539
Seismic response	111	1038
Seismology	118	1032
Response modification factors	121	1025
Ductility	98	853
Structural frames	83	689
Earthquakes	86	674

Reinforced concrete	77	635
Building codes	66	598
Structural design	80	557
Buildings	61	489
Seismic waves	42	359
Seismic performance	40	356
Structural analysis	44	328
Walls	35	320
Dynamic analysis	27	298
Earthquake engineering	30	291
Nonlinear analysis	31	280
Dynamic response	35	278
Tall buildings	46	276
Overstrength factor	31	255
Design	27	236
Ductility factor	24	221
Damping	31	220
Concrete buildings	27	219
Energy dissipation	27	218
Earthquake resistance	28	191
Finite element method	26	183
Pushover analysis	26	183
Push-over analysis	22	171
Ground motion	16	167
Nonlinearity	15	154
Static analysis	16	132

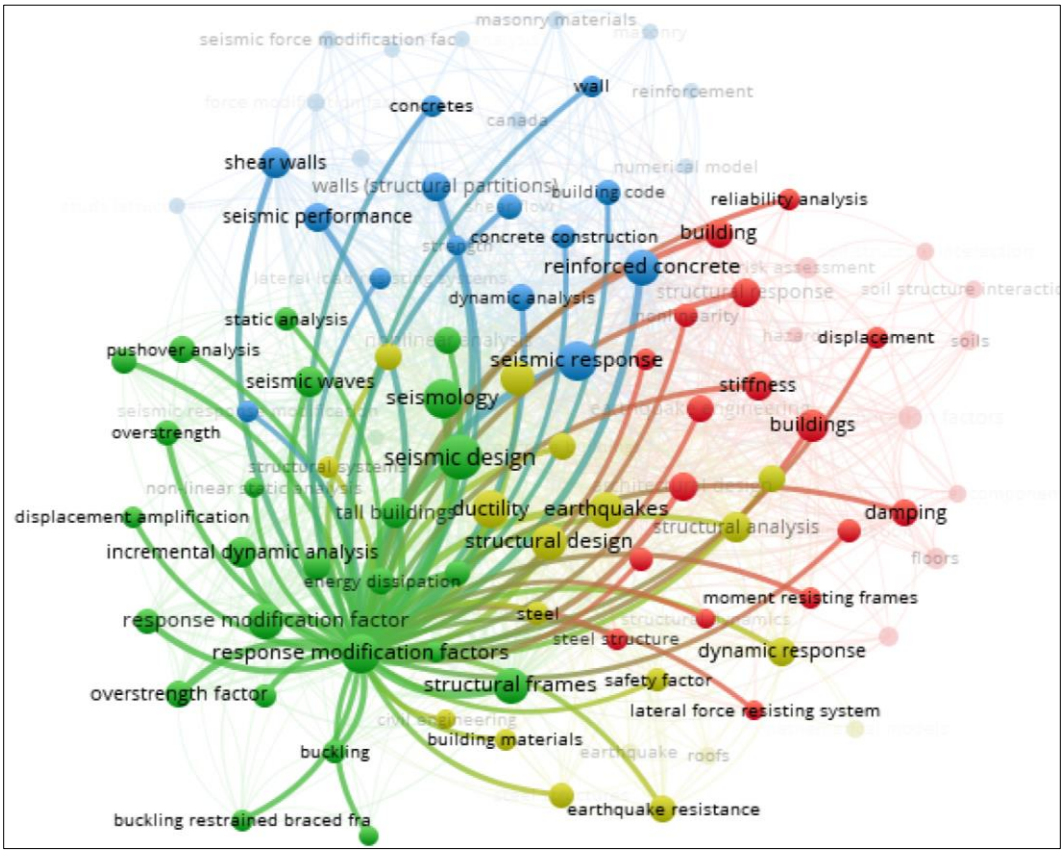

Figure 4. Example of the output in the VOSviewer (Item: Response modification factor, Cluster No. 2)

Table 2. Details of the main keywords

Item	Cluster No.#	Links	Total strength of links	Occurrences
Response Modification Factor	2	94	1025	121
Structural Frames	2	89	689	83
Buildings	1	86	489	61
Ductility	4	93	853	98
Reinforced Concrete	3	87	635	77
Seismic Performance	3	77	356	40
Seismic Design	2	96	1539	178

1.1. Identification of Response Modification Factor

This factor expresses the ability of a structure to sustain large deformations when subjected to lateral loads without a sudden post-peak drop in its strength [35]. Dissipation of large amounts of energy takes place in ductile buildings under lateral loads. The displacement ductility factor $R\mu$ (Equation 1) is defined by the ratio between failure displacements to yield displacements [11]. When calculating the ductility factors, the definition of the yield deformation often causes difficulty since the load-deformation relation may not have a well-defined yield point. This may occur due to the non-linear behavior of the materials or due to yielding of different parts of a structure commencing at different load levels.

$$Ductility\ factor\ (R_{\mu}) = \frac{\Delta_f}{\Delta_y} \quad (1)$$

where Δ_f is the failure displacement, and Δ_y is the yield displacement.

Various alternative definitions have been used by investigators to estimate the yield displacement and this research studies and presents two of those definitions.

Global Yield Method where the yield displacement (Δy) is the lateral displacement at 80% from ultimate load at ascending part of the curve while the failure displacement (Δf) is the lateral displacement at 80% from ultimate load at descending part of the curve. The ductility factor is computed using Equation 1 and Figure 5 shows the definition of failure displacement and yield displacement.

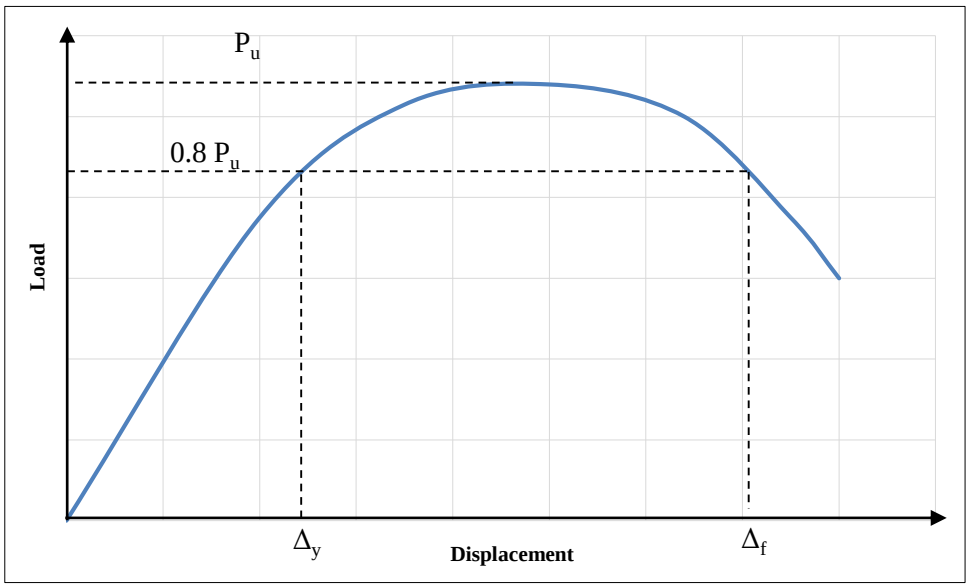

Figure 5. Failure displacement and yield displacement definitions [11]

First Yield Method, where the yield displacement (Δ_y) is the displacement when yielding first occurs in the system [36], while the failure displacement (Δ_f) is the lateral displacement at 80% from the ultimate load post peak. The ductility factor is computed using Equation 1.

The main objective of this research is to study the global performance of masonry-infilled reinforced concrete frame structures under lateral loading [37] and the influence of masonry-infilled wall distribution on the ductility of buildings. And for the fulfillment of this objective, a number of buildings with regular and irregular wall distribution and with

different numbers of stories are investigated and compared with their corresponding bare-frame buildings via a series of nonlinear static pushover analyses using the Seismostruct program. Moreover, a comparison between the resulting ductility factors and their values in the different international codes is performed. The addressed international codes present the response modification factor as mentioned below in Table 3.

Table 3. The R factors values specified in different codes

Code	Seismic force-resisting system	Response Modification Coefficient, R
ASCE 7-22	Special reinforced concrete moment frames	8
	Intermediate reinforced concrete moment frames	5
	Ordinary reinforced concrete moment frames	3
Uniform Building Code 97	Concrete special moment-resisting frame (SMRF)	8.5
	Concrete intermediate moment-resisting frame (IMRF)	5.5
	Concrete ordinary moment-resisting frame (OMRF)	3.5
SBC 301-18	Special reinforced concrete moment frames	6.5
	Intermediate reinforced concrete moment frames	4
	Ordinary reinforced concrete moment frames	2.5
Egyptian Code	Ordinary reinforced concrete moment frames	5

The main objective of this research is to develop the effect of masonry infills and their distribution on the lateral behavior of reinforced concrete medium-rise skeletal buildings. For this purpose, a parametric study was performed on five, seven, and ten-story' buildings that are modeled as bare and infilled frames, as shown in Figure 6. Infill ratio, panel aspect ratio, unidirectional eccentricity, and bidirectional eccentricities were the parameters investigated. The proposed model with different wall configurations is illustrated and investigated in Section 2. The results of the static pushover analyses on all models, along with the deduced equations for the ductility factor, are discussed in Section 3. See the detailed process in the diagram in Figure 7.

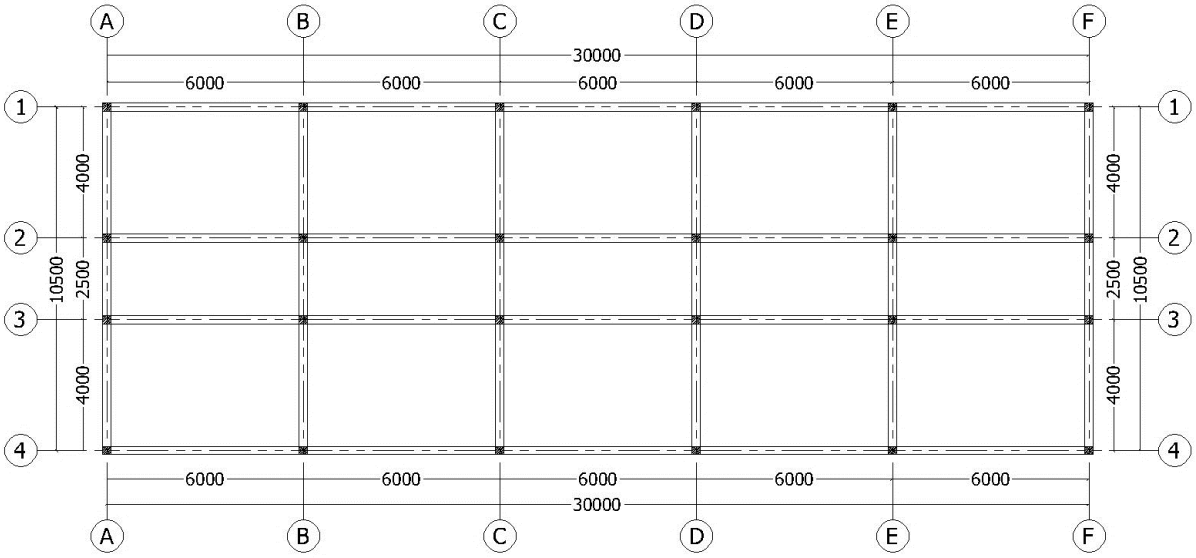

Figure 6. Plan showing the geometry of each floor of the three buildings (all dimensions are in mm)

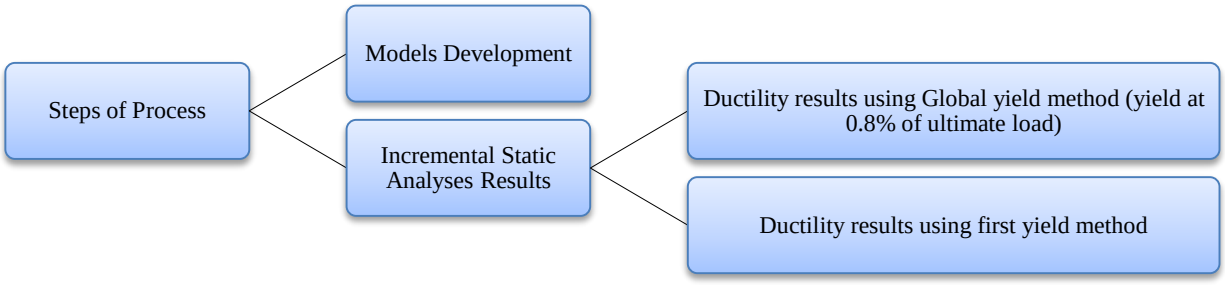

Figure 7. Steps of the work

2. Models Development

Firstly, according to Helmy et al. [38], the model was discussed and analyzed. The model consisted of five-story, seven-story, and ten-story reinforced concrete-infilled frames of a plan shown in Figure 7, and all dimensions are in mm. The different models, together with a bare frame model, are displayed in Table 4, along with the varied infill panel designs and infill ratios used to model each building. The structural elements (beams and columns) were modeled as inelastic frame elements [39, 40], which are capable of modeling members of space frames with geometric and material nonlinearities, with a fixed support condition being provided at the base of all columns, beam column joints being rigidly connected, and the beam column joints being rigidly connected.

Table 4. Analyzed models with different walls distribution throughout the plan

FE Analysis Matrix For Infilled Frames Buildings													
ID	MODEL	STORIES	Y-Frames				X-Frames						Description
			1-1	2-2	3-3	4-4	A-A	B-B	C-C	D-D	E-E	F-F	
1	CTRL	5,7,10	FFFFF*	FFFFF	FFFFF	FFFFF	FFF	FEF**	FEF	FEF	FEF	FFF	Control
2	T1Y	5,7,10	FFFFF	FFFFF	FFFFF	FFFFF	FFF	EEE	EEE	EEE	EEE	FFF	Translational
3	T2Y	5,7,10	FFFFF	FFFFF	FFFFF	FFFFF	FFF	FEF	EEE	EEE	FEF	FFF	Translational
4	T3Y	5,7,10	FFFFF	FFFFF	FFFFF	FFFFF	FFF	EEE	FEF	FEF	EEE	FFF	Translational
5	E1X	5,7,10	FFFFF	FFFFF	FFFFF	FFFFF	FFF	FEF	FEF	FEF	EEE	FFF	Torsional
6	E2X	5,7,10	FFFFF	FFFFF	FFFFF	FFFFF	FFF	FEF	FEF	EEE	EEE	FFF	Torsional
7	E3X	5,7,10	FFFFF	FFFFF	FFFFF	FFFFF	FFF	FEF	EEE	EEE	EEE	FFF	Torsional
8	T1X	5,7,10	FFFFF	FFEFF	FFEFF	FFFFF	FFF	FEF	FEF	FEF	FEF	FFF	Translational
9	T2X	5,7,10	FFFFF	FEEEF	FEEEF	FFFFF	FFF	FEF	FEF	FEF	FEF	FFF	Translational
10	E1XY	5,7,10	FFFFF	FFFFF	FFEFF	FFFFF	FFF	FEF	FEF	EEE	FEF	FFF	Torsional
11	E2XY	5,7,10	FFFFF	FFFFF	FFEFF	FFFFF	FFF	FEF	FEF	EEE	EEE	FFF	Torsional
12	E3XY	5,7,10	FFFFF	FFFFF	FEEEF	FFFFF	FFF	FEF	FEF	EEE	FEF	FFF	Torsional
13	E4XY	5,7,10	FFFFF	FFFFF	FEEEF	FFFFF	FFF	FEF	FEF	EEE	EEE	FFF	Torsional

*F = Infilled Frame, **E = Bare Frame

The control and translational mode buildings are the models with symmetrical walls' distribution throughout the story with various wall configurations, whereas the torsional mode buildings are the models with asymmetrical walls' distribution throughout the story with various wall configurations. Table 4 shows how masonry infill walls are distributed throughout the usual story of each model (building) with various numbers of stories.

SeismoStruct is a finite element tool for structural analysis that can forecast how large displacements would behave for 3D frames under static or dynamic loadings while taking geometry nonlinearities and material inelastic properties into account. The four-node masonry panel element used to represent the infill masonry has six struts per panel. According to Figure 8, each diagonal in both directions displays two parallel struts with lengths (dm) that range from 3.9 to 6.7 m and widths equal to 0.25 m for the infill panels with aspect ratios (the aspect ratio = length/height) that range from 0.833 to 2 depending on where the structural member is located in the plan, as shown in Figure 6, and a third vertical one that carries the shear from the top to the bottom of the panel (Figure 8). The strut only functions at the diagonal, which is compressed as a result of lateral loads, and its activation depends on the panel's deformation. The vertical shear strut follows a specialized bilinear hysteresis rule, whereas the diagonal struts adhere to the masonry strut hysteresis model [38].

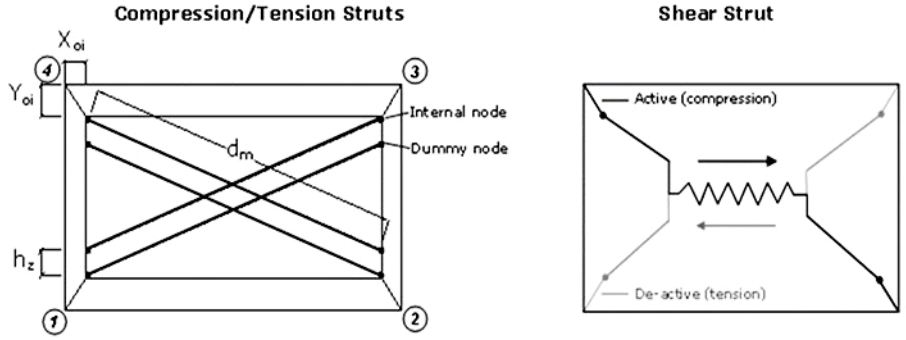

Figure 8. Infilled panel model

The infill panels have an aspect ratio (length/height) that varies from 0.833 to 2 depending on the location of the panel in the plan (Figure 6). Each model of a building was subjected to incremental horizontal loads distributed linearly with the height of the building from 0 (at the bottom) to 10 kN (at the top) in the X-direction, as illustrated in Figure 9, in addition to permanent gravity actions. All columns in all models were fixedly supported at the bottom. All structures subject to lateral loads have undergone a series of incremental static assessments; the findings are analyzed and presented.

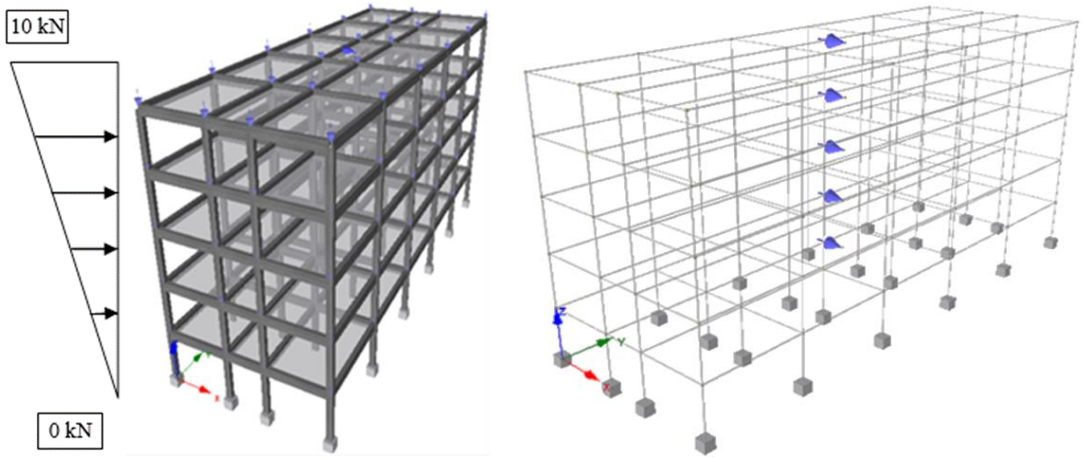

Figure 9. Loading on all models

The beam section was 250 mm wide and 500 mm deep for all models (5-story, 7-story, and 10-story models), the slab was 100 mm thick, and the infill was 250 mm thick. However, for 5-story, 7-story, and 10-story buildings, respectively, the cross sections of the columns were 250×400 mm, 250×500 mm, and 300×550 mm. Bricks and mortar make up the masonry infill, yet it is modeled as strut members. Concrete's tensile strength was 3 MPa while its compressive strength was 30 MPa, and the yield strength of steel's reinforcement was 360 MPa while its modulus of elasticity was 200 GPa. The structural elements were designed using SAP 2000, and the masonry's specific weight was 18 kN/m^3. The typical floor that was suggested was modeled and loaded with live loads of 3 kN/m^2 and floor cover loads of 2 kN/m^2. Thus, in order to reinforce all beams in the various structures mentioned above, 3 bars of 12 mm diameter (lower reinforcement) and 2 bars of 12 mm diameter (upper reinforcement) were designed; for the reinforcement of columns, 4, 6, and 8 bars of 18 mm diameter were designed, respectively, for 5, 7, and 10-story buildings. In all models, the storey height was kept at three meters throughout the several storey levels. A series of incremental static analyses have been conducted on all structures under lateral loads, and the results obtained are discussed and shown.

3. Incremental Static Analyses Results

A displacement-based nonlinear static analysis [41] was employed with an inverted triangular lateral-load distribution to obtain the capacity curves of each building. The energy resulted by the earthquake can be dissipated in well-confined regions like beam ends and column bases; because of that, the beam sway technique is the most preferable failure technique [42]. Subsequently, the columns of the building will be protected from serious damage during strong ground motions. Moreover, the plastic hinges formed in the elements of the frame in frame structures have high rotational ductility and do not experience sudden strength and stiffness degradation during earthquakes, causing an increase in the ductility of the building and a stable behavior under cyclic loading [43]. In contrast to the bare frame, the masonry-infilled frame shows a localized damage pattern. From the resulted performance of the different models, the first story always exhibits the first crack (damage), and its columns experience severe damage. This damage may be due to the inability of the infill panels to handle the redistribution of the structure strength after the first damage. So, infill panels must be considered in the design process so that the redistribution of the strength in the structure under lateral loading can meet the seismic demand for each story.

3.1. Ductility Results Using Global Yield Method (Yield at 0.8% of Ultimate Load)

The percentage of infills in the Y direction is defined by the ratio between the total lengths of infills in the Y direction and the total lengths of frames in the same direction, while the percentage of infills in the X direction is defined by the ratio between the total lengths of infills in the X direction and the total lengths of frames in the same direction.

The ductility factor varies with respect to the percentage of infills and the wall configurations in each building, so it's not accurate to specify a certain value for each system (see Figures 10 and 11). Whereas for control and translational mode 5-story buildings with regular wall distribution, the ductility factor decreases by 18.5% with an increase of infill

ratio by 25.4% and decreases by 84% with an increase of infill ratio by 50.79%, while for 7-story buildings with regular wall distribution, the ductility factor decreases by 26% with the increase of infill ratio by 25.4% and decreases by 55% with the increase of infill ratio by 50.79%, and for 10-story buildings with regular wall distribution, the ductility factor decreases by 34% with the increase of infill ratio by 25.4% and decreases by 67% with the increase of infill ratio by 50.79%. As shown in Figure 10, with respect to the Egyptian code of practice [44], the percentage of variance of the ductility values has reached 398 percent, while with respect to the uniform building code [45], it has reached 569 percent, and with respect to the American society of civil engineering [46], it has reached 664 percent, while with respect to the Saudi standard building code, it has reached 796 percent [47].

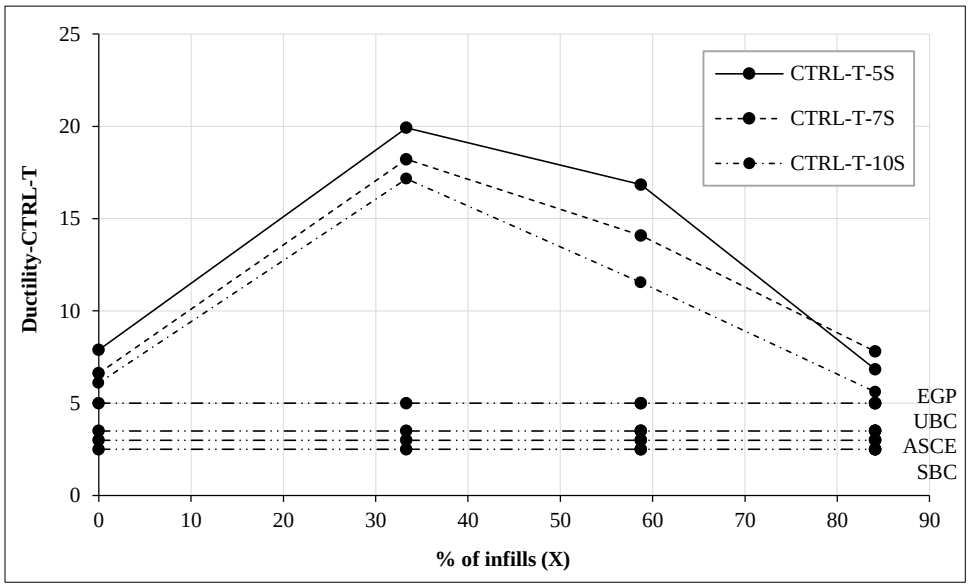

Figure 10. The effect of infills on the ductility factor in X-direction for five-story, seven-story, ten-story buildings

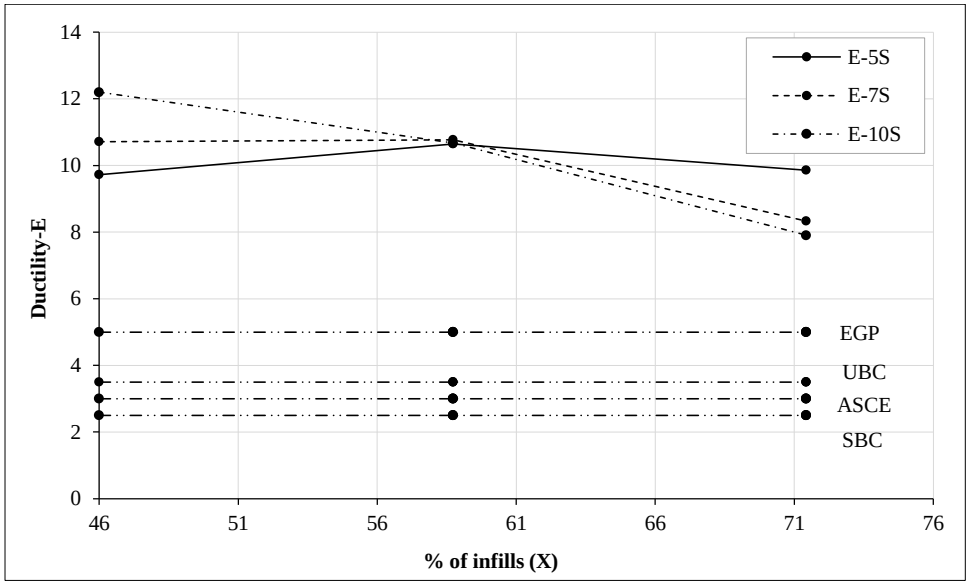

Figure 11. The effect of infills on the ductility factor in X-direction for five-story, seven-story, ten-story buildings

On the other hand, for 5-story buildings with irregular wall distribution (Figure 11), the ductility factor decreases by 20.89% with the increase of infill ratio by 12.73% and decreases by 27.4% with the increase of infill ratio by 25.43%, while for 10-story buildings with irregular wall distribution, the ductility factor decreases by 23% with the increase of infill ratio by 12.73% and decreases by 38% with the increase of infill ratio by 25.43%. From Figure 11, it can be concluded that the similarity in wall distribution throughout the story increases the ductility factor by approximately 143%, that the torsional effect causes excessive ductility demands on the structure, and that the ductility factor decreases in higher structures. And with respect to the Egyptian code of practice, the percentage of variance of the ductility values has reached 292 %, while with respect to the uniform building code, it has reached 417 %, and with respect to the American society of civil engineering, it has reached 486 %, while with respect to the standard building code, it has reached 584 %.

3.2. Ductility Results Using First Yield Method

A comparison is performed between the results of the ductility factor as a function of the percentage of infills and the percentage of eccentricity from both methods, the global yield method and the first yield method, showing that the values of the ductility resulted from the global yield method are unreasonable. The comparison is illustrated using the software MATLAB in Figure 12.

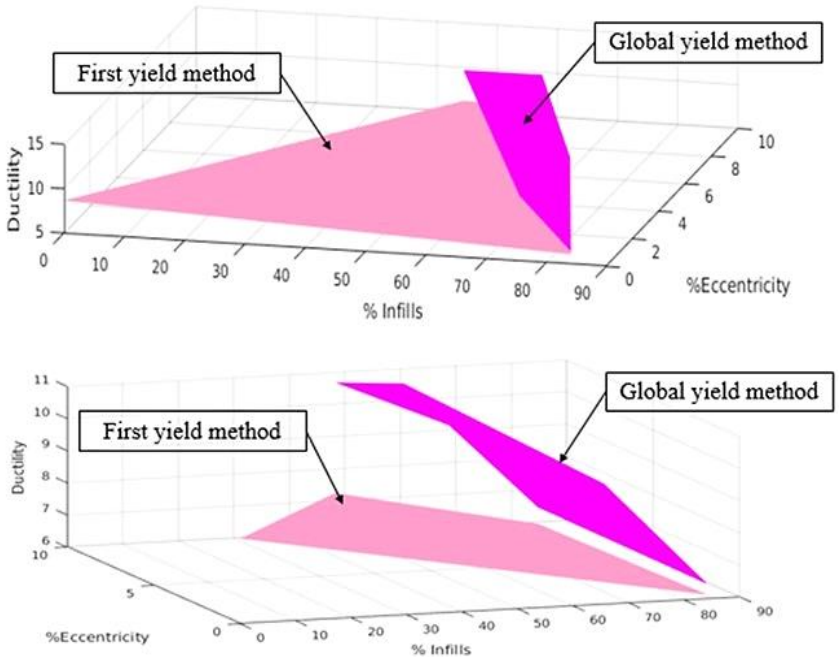

Figure 12. A 3-D chart illustrating the difference between the ductility factors resulted from both the global yield method and the first yield method as a function of the % of infills and the % of eccentricity

Also, as shown in Tables 5 and 6, and by comparing the ductility results of the first method (yield displacement at 0.8 of the ultimate load) and the second method (yield displacement at the first yield in the structure), it can be concluded that the results of the second method are more reasonable than those of the first one and that it's too conservative to consider the yield displacement at 80% of the ultimate load at the ascending part while studying the behavior of a whole structure. As shown in the results, for the majority of models, this displacement happened before the structure reached the yield point. Thus, this displacement cannot signify the yield of the structure. So, the general equations shown in Figures 13 to 15 for the ductility factor will be deducted from the first yield method as a function of the infill ratio for symmetrical and unsymmetrical wall distribution models.

Table 5. Resulted ductility from static pushover analysis for all models

No. of Stories	Models	% of infills (Y)*	% of infills (X)**	$\Delta_{0.8u}$	Δ_y	$R_\mu = \Delta_{0.8u}/\Delta_y$
5 STORIES	NO INFILL	0	0	0.487	0.06166	7.898
	CTRL-5S	100	84.127	0.2776	0.05167	5.372
	T1X	90	84.127	0.23	0.029	7.931
	T2X	70	84.127	0.23	0.032	7.187
	T1Y	100	33.33	0.267	0.0134	19.925
	T2Y	100	58.73	0.2274	0.014	16.242
	T3Y	100	58.73	0.2269	0.013	17.453
	E1X	100	71.43	0.206	0.02875	7.165
	E2X	100	58.73	0.19996	0.026	7.690
	E3X	100	46	0.1945	0.02	9.725
	E1XY	95	71.43	0.22	0.015	14.666
	E2XY	95	58.73	0.19	0.017	11.176
	E3XY	85	71.43	0.2285	0.0295	7.745
	E4XY	85	58.73	0.196	0.015	13.066

7 STORIES	NO INFILL	0	0	0.52	0.0785	6.624
	CTRL-7S	100	84.127	0.37167	0.0447	8.314
	T1X	90	84.127	0.244	0.03	8.133
	T2X	70	84.127	0.3033	0.0434	6.988
	T1Y	100	33.33	0.3333	0.0183	18.213
	T2Y	100	58.73	0.284	0.021	13.523
	T3Y	100	58.73	0.293	0.02	14.65
	E1X	100	71.43	0.275	0.034	8.088
	E2X	100	58.73	0.262	0.02	13.1
	E3X	100	46	0.3	0.028	10.714
	E1XY	95	71.43	0.277	0.021	13.19
	E2XY	95	58.73	0.264	0.025	10.56
	E3XY	85	71.43	0.08	0.0214	3.738
	E4XY	85	58.73	0.264	0.0305	8.655
10 STORIES	NO INFILL	0	0	0.599	0.0982	6.099
	CTRL-10S	100	84.127	0.2635	0.046	5.728
	T1X	90	84.127	0.262	0.05	5.24
	T2X	70	84.127	0.3	0.051	5.882
	T1Y	100	33.33	0.41167	0.024	17.152
	T2Y	100	58.73	0.341	0.03	11.366
	T3Y	100	58.73	0.34	0.029	11.724
	E1X	100	71.43	0.28	0.037	7.567
	E2X	100	58.73	0.3455	0.0366	9.439
	E3X	100	46	0.354	0.029	12.206
	E1XY	95	71.43	0.33154	0.0416	7.969
	E2XY	95	58.73	0.343	0.0317	10.82
	E3XY	85	71.43	0.32	0.039	8.205
	E4XY	85	58.73	0.341	0.029	11.758

Table 6. Resulted ductility from static pushover analysis for all models

No. of Stories	Models	% of infills(Y)*	% of infills(X)**	$\Delta_{0.8u}$	Δ_{yb}	$R_\mu = \Delta_{0.8u}/\Delta_{yb}$
5 STORIES	NO INFILL	0	0	0.49	0.05	9.8
	CTRL-5S	100	84.127	0.2776	0.047	5.906
	T1X	90	84.127	0.23	0.026	8.846
	T2X	70	84.127	0.23	0.035	6.571
	T1Y	100	33.33	0.267	0.043	6.21
	T2Y	100	58.73	0.2274	0.029	7.841
	T3Y	100	58.73	0.2269	0.033	6.875
	E1X	100	71.43	0.205	0.0211	9.7
	E2X	100	58.73	0.199	0.0206	9.66
	E3X	100	46	0.1945	0.02	9.72
	E1XY	95	71.43	0.22	0.0235	9.36
	E2XY	95	58.73	0.19	0.029	6.55
	E3XY	85	71.43	0.228	0.016	7.6
	E4XY	85	58.73	0.196	0.0225	8.71

7 STORIES	NO INFILL	0	0	0.52	0.06	8.67
	CTRL-7S	100	84.127	0.3716	0.043	8.64
	T1X	90	84.127	0.244	0.046	5.304
	T2X	70	84.127	0.3	0.035	8.57
	T1Y	100	33.33	0.3333	0.048	6.937
	T2Y	100	58.73	0.284	0.045	6.311
	T3Y	100	58.73	0.293	0.047	6.234
	E1X	100	71.43	0.275	0.039	7.05
	E2X	100	58.73	0.262	0.0482	5.435
	E3X	100	46	0.3	0.048	6.25
	E1XY	95	71.43	0.277	0.0433	6.397
	E2XY	95	58.73	0.264	0.0464	5.689
	E3XY	85	71.43	0.08	0.0357	2.24
	E4XY	85	58.73	0.26	0.03	8.6
10 STORIES	NO INFILL	0	0	0.599	0.08	7.5
	CTRL-10S	100	84.127	0.2635	0.07	3.764
	T1X	90	84.127	0.262	0.073	3.589
	T2X	70	84.127	0.3	0.061	4.918
	T1Y	100	33.33	0.41167	0.056	7.14
	T2Y	100	58.73	0.341	0.06	5.683
	T3Y	100	58.73	0.34	0.061	5.573
	E1X	100	71.43	0.28	0.0612	4.571
	E2X	100	58.73	0.345	0.0595	5.798
	E3X	100	46	0.354	0.0555	6.378
	E1XY	95	71.43	0.33	0.0653	5.053
	E2XY	95	58.73	0.343	0.0566	6
	E3XY	85	71.43	0.32	0.05	6.4
	E4XY	85	58.73	0.341	0.05	6.8

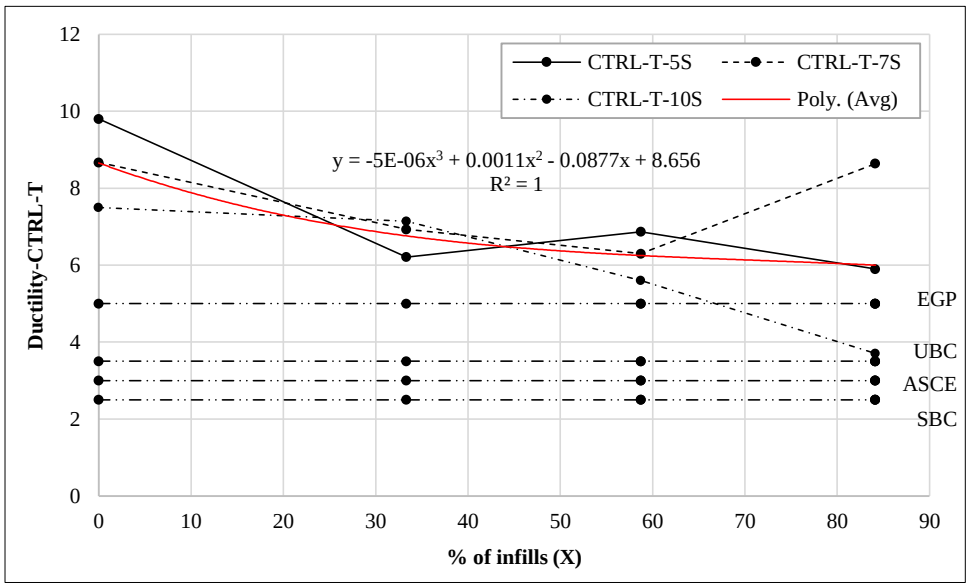

Figure 13. The effect of infills on the ductility factor in X-direction for five-story, seven-story, ten-story buildings and a general equation to determine the ductility factor for symmetrical medium rise buildings

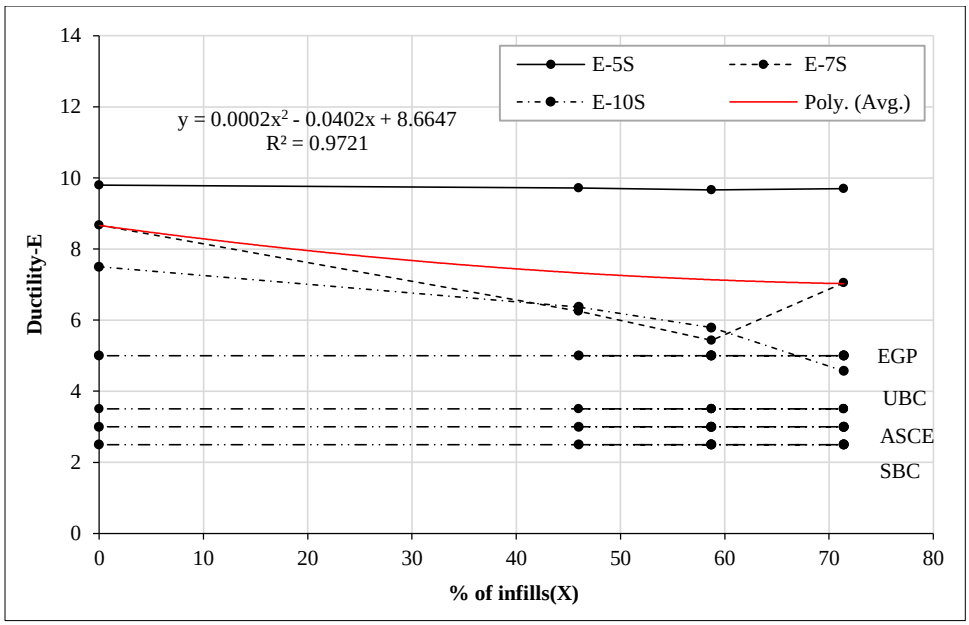

Figure 14. The effect of infills on the ductility factor in X-direction for unsymmetrical five-story, seven-story, ten-story buildings and a general equation to determine the ductility factor for unsymmetrical medium rise buildings as a function of the percentage of infills in X-direction.

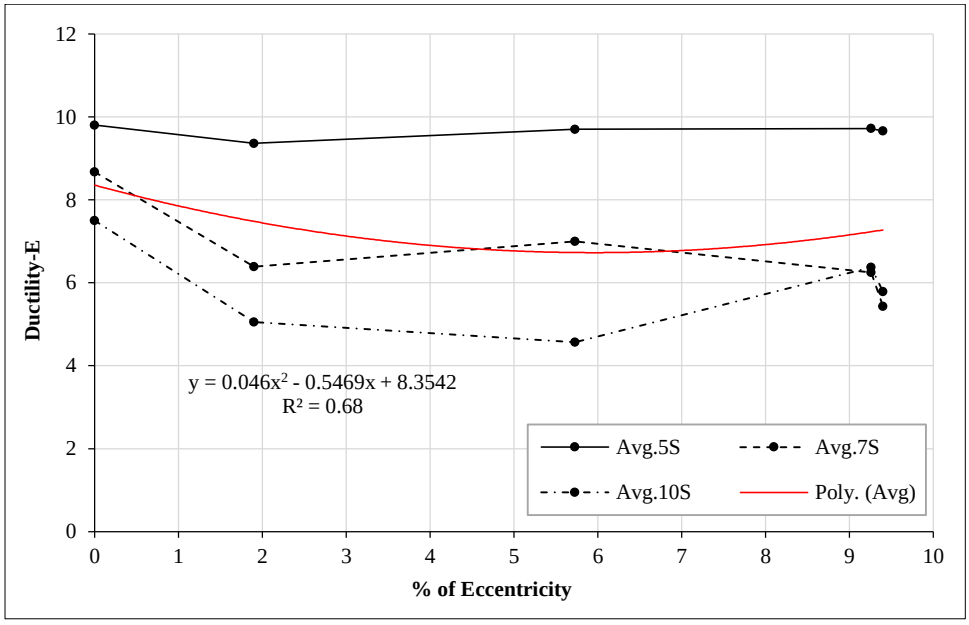

Figure 15. A general equation to determine the ductility factor for unsymmetrical medium rise buildings as a function of the eccentricity of different walls distributions throughout the plan

These equations are concluded from the ductility results of buildings (models) with the same infill ratio in the Y direction (100% infill) but a different infill ratio in the X direction (the load direction). Thus, the response modification factor can be displayed in the national and international codes as an equation instead of a fixed value. It depends on the percentage of infill in the building and the irregularity of the plan. Equation 2 presents the ductility factor as a function of the percentage of infills for symmetrical plans, and Equation 3 as well as Equation 4 present the ductility factor as a function of the percentage of infills and the percentage of eccentricity in unsymmetrical plans.

$$y = -5E\text{-}06x^3 + 0.0011x^2 - 0.0877x + 8.656 \quad (2)$$

$$y = 0.0002x^2 - 0.0402x + 8.6647 \quad (3)$$

$$y = 0.046x^2 - 0.5469x + 8.3542 \quad (4)$$

4. Conclusions

An analytical study of the seismic response of infilled-frame buildings was reported in this research. Different storey numbers and infill distribution patterns were used to assess several prototype building types. This investigation's main finding is the deduction of an equation to calculate the response modification factor (ductility factor) for a building, expressed as the ratio between the maximum deformation resulted from lateral loading and the corresponding yield deformation, depending on the percentage of infills inside that building as well as its distribution throughout the plan. Using fixed values for the ductility factor was shown to be unreasonable, and this could result in excessively conservative designs for the ductile building structures.

The analytical results showed that the ductility factor depends highly on the percentage of infills in the structure and its distribution in the plan, as there is an inversely proportional relationship attributed to the added stiffness contribution of the infills to the bare frames. It can be concluded that the ductility factors of the buildings with symmetrical wall distribution were greater than the ductility factors of the buildings with unsymmetrical wall distribution by a percentage that reached 207% for buildings with the same infill ratio. Furthermore, a comparison between the resulted values for the ductility factor and its values in national and international codes was performed, and the percentage of variance has reached values as high as 796% for symmetrical plan buildings and 584 % for unsymmetrical plan buildings.

Even though not all potential elements influencing the seismic response of infilled-frame buildings were examined in this study, it is obvious that the response modification factors included in national and international codes need to be reviewed. Given the system's innate strength and ductility, the margin of overestimation of the seismic forces is now seen as significant. If the response modification parameters are related to infill percentages and distributions, this will result in more effective and economic designs.

The following are proposed for further studies:

- To generalize the results of this research, other building plans and layouts and other wall configurations might be presented and studied.
- Dynamic time history analyses should be performed on buildings to obtain a more accurate representation of the earthquake ground motions; thus, the results will be more precise.
- Study other factors that affect the seismic response of infilled frame structures, such as the overstrength factor and the deflection amplification factor. Also, the rotation of members can help investigate the fragility of the structure.
- Study the influence of considering the contribution of infill walls in resisting lateral loads during the design process on the construction cost of the buildings.

5. Declarations

5.1. Author Contributions

Conceptualization, H.O.; methodology, H.O.; software, D.H.; validation, M.Z. and H.O.; formal analysis, D.H.; investigation, D.H.; resources, H.O.; data curation, D.H.; writing—original draft preparation, D.H.; writing—review and editing, H.O.; visualization, M.Z.; supervision, M.Z. All authors have read and agreed to the published version of the manuscript.

5.2. Data Availability Statement

The data presented in this study are available in the article.

5.3. Funding

The authors received no financial support for the research, authorship, and/or publication of this article.

5.4. Conflicts of Interest

The authors declare no conflict of interest.

6. References

[1] Shing, P. B., & Mehrabi, A. B. (2002). Behaviour and analysis of masonry-infilled frames. Progress in Structural Engineering and Materials, 4(3), 320–331. doi:10.1002/pse.122.

[2] Ahmed, A., Ali, A., Khalid, H., & Ahmad, M. (2018). Role of masonry infill wall on the seismic behavior of typical four-storey building in Pakistan. IOP Conference Series: Materials Science and Engineering, 414, 012017. doi:10.1088/1757-899x/414/1/012017.

[3] Silva, L. M., Vasconcelos, G., & Lourenço, P. B. (2021). Innovative systems for earthquake-resistant masonry infill walls: Characterization of materials and masonry assemblages. Journal of Building Engineering, 39, 102195. doi:10.1016/j.jobe.2021.102195.

[4] Elhegazy, H., Ebid, A., Mahdi, I. M., Haggag, S. Y. A., & Rashid, I. A. (2021). Decision Making and Predicting the Cost for the Optimal Structural System of Multi-Story Buildings. American Journal of Engineering and Applied Sciences, 14(2), 152–161. doi:10.3844/ajeassp.2021.152.161.

[5] Elhegazy, H., Ebid, A., AboulHaggag, S., Mahdi, I., & AbdelRashid, I. (2023). Cost optimization of multi-story steel buildings during the conceptual design stage. Innovative Infrastructure Solutions, 8(1), 36. doi:10.1007/s41062-022-00999-2.

[6] Murty, C. V. R., & Jain, S. K. (2000). Beneficial influence of masonry infill walls on seismic performance of RC frame buildings. 12th World Conference on Earthquake Engineering, 30 January-4 February, Auckland, New Zealand.

[7] Falcão Moreira, R., Varum, H., & Castro, J. M. (2023). Influence of Masonry Infill Walls on the Seismic Assessment of Non-Seismically Designed RC Framed Structures. Buildings, 13(5), 1148. doi:10.3390/buildings13051148.

[8] Kauffman, A., & Memari, A. M. (2014). Performance evaluation of different masonry infill walls with structural fuse elements based on in-plane cyclic load testing. Buildings, 4(4), 605–634. doi:10.3390/buildings4040605.

[9] Tamboli, H., & Karadi, U. (2012). Seismic Analysis of RC Frame Structure with and without Masonry Infill Walls. Indian Journal of Natural Sciences, 3(14), 1137–1148.

[10] Dias-Oliveira, J., Rodrigues, H., Asteris, P. G., & Varum, H. (2022). On the Seismic Behavior of Masonry Infilled Frame Structures. Buildings, 12(8), 1146. doi:10.3390/buildings12081146.

[11] Tawfik Essa, A. S. A., Kotp Badr, M. R., & El-Zanaty, A. H. (2014). Effect of infill wall on the ductility and behavior of high strength reinforced concrete frames. HBRC Journal, 10(3), 258–264. doi:10.1016/j.hbrcj.2013.12.005.

[12] Furtado, A., Vila-Pouca, N., Varum, H., & Arêde, A. (2019). Study of the seismic response on the infill masonry walls of a 15-storey reinforced concrete structure in Nepal. Buildings, 9(2), 39. doi:10.3390/buildings9020039.

[13] Mohamed, W. A. E.-W. (2012). Parametric Study on the Effect of Masonry Infill Walls on the Seismic Resistance of RC Buildings. JES: Journal of Engineering Sciences, 40(3), 701–721. doi:10.21608/jesaun.2012.114405.

[14] Balun, B. (2023). The influence of ground motion duration on the energy based assessment of buildings with infill walls. Structures, 49, 765–778. doi:10.1016/j.istruc.2023.02.011.

[15] Hareen, C. H. B. V., & Mohan, S. C. (2021). Evaluation of seismic torsional response of ductile RC buildings with soft first story. Structures, 29, 1640–1654. doi:10.1016/j.istruc.2020.12.031.

[16] Qian, K., Lan, D. Q., Li, S. K., & Fu, F. (2021). Effects of infill walls on load resistance of multi-story RC frames to mitigate progressive collapse. Structures, 33, 2534–2545. doi:10.1016/j.istruc.2021.06.015.

[17] Uprety, R., & Suwal, R. (2023). Bidirectional effect of earthquake on low-rise RC frames with and without the consideration of In-plane effect of unreinforced masonry infill. Structures, 47, 648–664. doi:10.1016/j.istruc.2022.11.099.

[18] Lata, A., Xun, G., Ruofan, L., Xiaoyao, D., & Bideng, L. (2022). Experimental study on the seismic performance of RC frames considering the cast sequence of infilled walls and columns. Structures, 44, 186–199. doi:10.1016/j.istruc.2022.08.006.

[19] Baniahmadi, M., Vafaei, M., & C Alih, S. (2022). Cyclic response of reinforced concrete frames partially infilled with relatively weak masonry wall. Journal of Building Engineering, 46, 103722. doi:10.1016/j.jobe.2021.103722.

[20] Papasotiriou, A., Athanatopoulou, A., & Kostinakis, K. (2021). Parametric study of the masonry infills' effect on the seismic performance of R/C frames based on the use of different damage measures. Engineering Structures, 241, 112326. doi:10.1016/j.engstruct.2021.112326.

[21] Lyu, H., Deng, M., Han, Y., Ma, F., & Zhang, Y. (2022). In-plane cyclic testing of full-scale reinforced concrete frames with innovative isolated infill walls strengthened by highly ductile concrete. Journal of Building Engineering, 57, 104934. doi:10.1016/j.jobe.2022.104934.

[22] Elhegazy, H., Ebid, A., Mahdi, I., Haggag, S., & Abdul-Rashied, I. (2021). Implementing QFD in decision making for selecting the optimal structural system for buildings. Construction Innovation, 21(2), 345–360. doi:10.1108/CI-12-2019-0149.

[23] Elhegazy, H., Ebid, A. M., Mahdi, I. M., Aboul Haggag, S. Y., & Rashid, I. A. (2020). Selecting optimum structural system for R.C. multi-story buildings considering direct cost. Structures, 24, 296–303. doi:10.1016/j.istruc.2020.01.039.

[24] Pradhan, B., Zizzo, M., Sarhosis, V., & Cavaleri, L. (2021, October). Out-of-plane behaviour of unreinforced masonry infill walls: Review of the experimental studies and analysis of the influencing parameters. Structures, 33, 4387-4406. doi:10.1016/j.istruc.2021.07.038.

[25] Kong, J., Su, Y., Zheng, Z., Wang, X., & Zhang, Y. (2022). The Influence of Vertical Arrangement and Masonry Material of Infill Walls on the Seismic Performance of RC Frames. Buildings, 12(6), 825. doi:10.3390/buildings12060825.

[26] FEMA P-695. (2009). Quantification of building seismic performance factors: Component Equivalency Methodology. Federal Emergency management Agency (FEMA), Washington, United States.

[27] Fazileh, F., Khosravi, S., Dolati, A., Fathi-Fazl, R., & Saatcioglu, M. (2022). Seismic performance assessment of conventional construction concrete moment-resisting frame buildings in Canada using the FEMA P695 methodology. Canadian Journal of Civil Engineering, 49(9), 1508–1517. doi:10.1139/cjce-2021-0603.

[28] Fischer, A. W., & Schafer, B. W. (2023). Wall-diaphragm interactions in seismic response of building systems ii: Inelastic response and design. Earthquake Engineering and Structural Dynamics, 52(5), 1557–1577. doi:10.1002/eqe.3829.

[29] Gul, A., Alam, B., & Shahzada, K. (2022). Seismic performance evaluation of unconfined dry stacked block masonry structure. Engineering Structures, 265, 114529. doi:10.1016/j.engstruct.2022.114529.

[30] Nasr, N. E., Fayed, M. N., Hussien, G., & El-Makhlasawi, A. M. (2022). The Effect of Shear Wall Openings on the Response Reduction Factor. Civil Engineering Journal (Iran), 8(4), 796–822. doi:10.28991/CEJ-2022-08-04-013.

[31] Ehteshami Moeini, M., Razavi, S. A., Yekrangnia, M., Pourasgari, P., & Abbasian, N. (2022). Cyclic performance assessment of damaged unreinforced masonry walls repaired with steel mesh reinforced shotcrete. Engineering Structures, 253, 113747. doi:10.1016/j.engstruct.2021.113747.

[32] Ricci, P., Di Domenico, M., & Verderame, G. M. (2019). Nonlinear Dynamic Assessment of the Out-Of-Plane Response and Behaviour Factor of Unreinforced Masonry Infills in Reinforced Concrete Buildings. Proceedings of the 7th International Conference on Computational Methods in Structural Dynamics and Earthquake Engineering (COMPDYN 2015), 2104-2115. doi:10.7712/120119.7062.19693.

[33] Ali, Q., Ahmad, N., Ashraf, M., & Schacher, T. (2022). Seismic Performance Evaluation of Two-story Dhajji-dewari Traditional Structure. International Journal of Architectural Heritage, 16(8), 1233–1251. doi:10.1080/15583058.2021.1875081.

[34] Liberatore, L., & AlShawa, O. (2021). On the application of the yield-line method to masonry infills subjected to combined in-plane and out-of-plane loads. Structures, 32, 1287–1301. doi:10.1016/j.istruc.2021.03.044.

[35] Shedid, M. T., El-Dakhakhni, W. W., & Drysdale, R. G. (2011). Seismic Response Modification Factors for Reinforced Masonry Structural Walls. Journal of Performance of Constructed Facilities, 25(2), 74–86. doi:10.1061/(asce)cf.1943-5509.0000144.

[36] Park, R. (1989). Evaluation of ductility of structures and structural assemblages from laboratory testing. Bulletin of the New Zealand Society for Earthquake Engineering, 22(3), 155–166. doi:10.5459/bnzsee.22.3.155-166.

[37] Asteris, P. G. (2008). Finite Element Micro-Modeling of Infilled Frames. Electronic Journal of Structural Engineering, 8, 1–11. doi:10.56748/ejse.894.

[38] Helmy, D. H. M., Okail, H., & Zidan, M. (2017). Evaluation of the Seismic Response Parameters for Infilled Reinforced Concrete Frame Buildings. IOSR Journal of Mechanical and Civil Engineering, 14(01), 28–41. doi:10.9790/1684-1401032841.

[39] Cavaleri, L., & Di Trapani, F. (2014). Cyclic response of masonry infilled RC frames: Experimental results and simplified modeling. Soil Dynamics and Earthquake Engineering, 65, 224–242. doi:10.1016/j.soildyn.2014.06.016.

[40] Caliò, I., & Pantò, B. (2014). A macro-element modelling approach of Infilled Frame Structures. Computers and Structures, 143, 91–107. doi:10.1016/j.compstruc.2014.07.008.

[41] Powell, G. H. (2008). Displacement-Based Seismic Design of Structures. Earthquake Spectra, 24(2), 555–557. doi:10.1193/1.2932170.

[42] Hosseinzadeh, S., & Galal, K. (2020). Seismic Fragility Assessment and Resilience of Reinforced Masonry Flanged Wall Systems. Journal of Performance of Constructed Facilities, 34(1). doi:10.1061/(asce)cf.1943-5509.0001383.

[43] Kakaletsis, D.J. (2012). Rotations of RC Members of Infilled Frames at Yielding and Ultimate. The Open Construction and Building Technology Journal, 6(1), 50–62. doi:10.2174/1874836801206010050.

[44] ECP-201. (2012) Egyptian Code of Practice for Calculation of Loads and Forces in Structures and Buildings. National Housing and Building Research Center, Cairo, Egypt.

[45] UBC-97. (1997). Structural Engineering Design Provisions. International Conference of Building Officials, Uniform Building Code, Whittier, United States.

[46] ASCE/SEI 7-22. (2022). Minimum Design Loads and Associated Criteria for Buildings and Other Structures. American Society of Civil Engineers (ASCE), Reston, United States.

[47] SBC 301-CR-18. (2018). Saudi Building Code Structural requirements for Loads and Forces. Saudi Building Code National Committee, Riyadh, Saudi Arabia.